

See discussions, stats, and author profiles for this publication at: <https://www.researchgate.net/publication/271535056>

One-Pot Synthesis of Imines from Nitroaromatics and Alcohols by Tandem Photocatalytic and Catalytic Reactions on Degussa (Evonik) P25 Titanium Dioxide

ARTICLE *in* ACS APPLIED MATERIALS & INTERFACES · JANUARY 2015

Impact Factor: 6.72 · DOI: 10.1021/am508769x · Source: PubMed

READS

44

9 AUTHORS, INCLUDING:



Kunlei Wang

Hokkaido University

3 PUBLICATIONS 1 CITATION

[SEE PROFILE](#)



Bunsho Ohtani

Hokkaido University

274 PUBLICATIONS 9,211 CITATIONS

[SEE PROFILE](#)



Satoshi Ichikawa

Osaka University

95 PUBLICATIONS 1,449 CITATIONS

[SEE PROFILE](#)



Shunsuke Tanaka

Kansai University

75 PUBLICATIONS 1,862 CITATIONS

[SEE PROFILE](#)

One-Pot Synthesis of Imines from Nitroaromatics and Alcohols by Tandem Photocatalytic and Catalytic Reactions on Degussa (Evonik) P25 Titanium Dioxide

Hiroaki Hirakawa,[†] Miyu Katayama,[†] Yasuhiro Shiraishi,^{*,†,‡} Hirokatsu Sakamoto,[†] Kunlei Wang,^{||} Bunsho Ohtani,^{||} Satoshi Ichikawa,[§] Shunsuke Tanaka,[⊥] and Takayuki Hirai[†]

[†]Research Center for Solar Energy Chemistry, and Division of Chemical Engineering, Graduate School of Engineering Science, and [§]Institute for NanoScience Design, Osaka University, Toyonaka 560-8531, Japan

[‡]PRESTO, JST, Saitama 332-0012, Japan

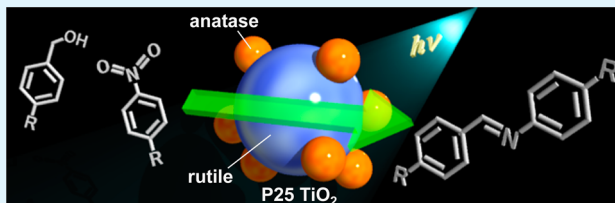
^{||}Catalysis Research Center, Hokkaido University, Sapporo 001-0021, Japan

[⊥]Department of Chemical, Energy and Environmental Engineering, Kansai University, Suita 564-8680, Japan

S Supporting Information

ABSTRACT: Photoirradiation ($\lambda > 300$ nm) of Degussa (Evonik) P25 TiO_2 , a mixture of anatase and rutile particles, in alcohols containing nitroaromatics at room temperature produces the corresponding imines with very high yields (80–96%). Other commercially available anatase or rutile TiO_2 particles, however, exhibit very low yields (<30%). The imine formation involves two step reactions on the TiO_2 surface: (i) photocatalytic oxidation of alcohols (aldehyde formation) and reduction of nitrobenzene (aniline formation) and (ii) condensation of the formed aldehyde and aniline on the Lewis acid sites (imine formation). The respective anatase and rutile particles were isolated from P25 TiO_2 by the $\text{H}_2\text{O}_2/\text{NH}_3$ and HF treatments to clarify the activity of these two step reactions. Photocatalysis experiments revealed that the active sites for photocatalytic reactions on P25 TiO_2 are the rutile particles, promoting efficient reduction of nitrobenzene on the surface defects. In contrast, catalysis experiments showed that the anatase particles isolated from P25 TiO_2 exhibit very high activity for condensation of aldehyde and aniline, because the number of Lewis acid sites on the particles ($73 \mu\text{mol g}^{-1}$) is much higher than that of other commercially available anatase or rutile particles ($<15 \mu\text{mol g}^{-1}$). The P25 TiO_2 particles therefore successfully promote tandem photocatalytic and catalytic reactions on the respective rutile and anatase particles, thus producing imines with very high yields.

KEYWORDS: photocatalysis, catalysis, titanium dioxide, Degussa (Evonik) P25, imines



INTRODUCTION

Aromatic imines are versatile intermediates for the synthesis of agricultural chemicals and pharmaceuticals.^{1,2} These imines are also very important electrophilic reagents for various reactions such as addition, cycloaddition, and condensation.^{3,4} They are usually synthesized by dehydrogenation of secondary amines;^{5,6} however, these methods require stoichiometric or excess amounts of strong oxidants such as *o*-iodoxybenzoic acid and MnO_2 and produce copious amount of wastes. Catalytic methods for dehydrogenation of secondary amines with molecular oxygen (O_2) as an oxidant have also been proposed;^{7–9} however, all of these methods require noble metal catalysts such as Ru, Pd, Pt, and Ir metals. Condensation of aldehydes and anilines is another method for imine synthesis, which proceeds at room temperature with Lewis acid catalysts.^{10–12} This method, however, suffers from low stability of substrates; both aldehydes and anilines are oxidized very easily by autoxidation by O_2 .⁷ Alternative methods for imine synthesis with stable substrates such as alcohols and nitroaromatics are therefore necessary for green organic synthesis.

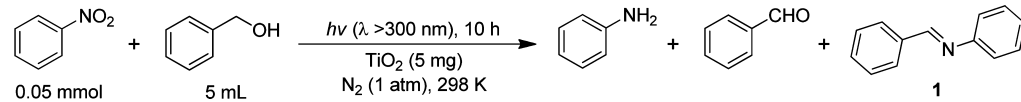
Some catalytic systems for imine synthesis with alcohols and nitroaromatics have been proposed.^{13–18} These systems promote three consecutive catalytic steps in one pot: (i) oxidation of alcohols into aldehydes, (ii) reduction of nitroaromatics to anilines, and (iii) condensation of the formed aldehydes and anilines (formation of imines). All of these systems, however, require high reaction temperatures (>373 K) and noble metal catalysts such as Ru complex,¹³ Ru hydroxide,¹⁴ Pd¹⁵ or Au nanoparticles,¹⁶ Ir–Pd,¹⁷ or Ir–Au dimetallic complexes.¹⁸ An one-pot catalytic system promoting efficient and selective imine synthesis without noble metals under milder reaction condition is highly desirable.

The purpose of the present work is to design a catalytic system that promotes *one-pot imine synthesis from alcohols and nitroaromatics without noble metals at room temperature*. We used a semiconductor titanium dioxide (TiO_2) as a catalyst under

Received: December 12, 2014

Accepted: January 26, 2015

Published: January 26, 2015

Table 1. One-Pot Synthesis of *N*-Benzylidenaniline (**1**) from Benzyl Alcohol and Nitrobenzene on Various TiO₂ under Photoirradiation^a

sample	catalyst	crystalline phase ^b	$S_{\text{BET}}/\text{m}^2 \text{ g}^{-1c}$	d_p/nm^d	nitrobenzene conv/% ^e	aniline yield/% ^e	benzaldehyde formed/ μmol^e	imine 1 yield/% ^e	$N_{\text{LA}}/\mu\text{mol g}^{-1f}$
1	JRC-TIO-1 ^g	A	73	16	34	<1	35	18	14.2
2	JRC-TIO-2 ^g	A	18	413	53	5	52	28	6.4
3	ST-41 ^h	A	11	160	63	46	72	16	2.0
4	CR-EL ^h	R	7	245	>99	72	125	24	<1
5	PT-101 ^h	R	25	71	>99	82	127	3	<1
6	JRC-TIO-6 ^g	R	100	21	>99	86	125	5	<i>i</i>
7	P25 ^{g,j}	A/R (83/17)	57	27,340	>99	<1	106	90	48.0
	first reuse				>99	<1	108	92	
	second reuse				>99	<1	107	89	
8	P25_anatase	A	67	27	71	3	74	56	73.3
9	P25_rutile	R	32	71	>99	63	123	16	3.4
10		A/R (80/20)			>99	<1	111	93	
11	P25_anatase/ P25_rutile ^k	A/R (90/10)			84	<1	78	72	
12		A/R (70/30)			>99	26	113	68	
13	JRC-TIO-1/JRC-TIO-6 ^l	A/R (80/20)			>99	<1	107	89	

^aPhotoirradiation was carried out with a 2 kW Xe lamp (light intensity at 300–450 nm is 27.3 W m⁻²). ^bDetermined by XRD analysis, where the ratio of anatase (A) and rutile (R) was determined with the equation; A (%) = $I_{\text{A}(101)} / (I_{\text{A}(101)} + 1.4I_{\text{R}(110)}) \times 100$.²⁴ ^cBET surface area determined by N₂ adsorption/desorption analysis. ^dParticle diameter determined by DLS analysis. ^eDetermined by GC analysis. ^fThe number of Lewis acid sites per gram TiO₂, measured by pyridine adsorption analysis. ^gJapan Reference Catalyst supplied from the Catalyst Society of Japan. ^hSupplied from Ishihara Sangyo, Ltd. (Japan). ⁱCannot be determined because a strong absorption band, assigned to the pyridine adsorbed onto the Ti³⁺ atoms on a large number of surface defects, appears at 1441 cm⁻¹ and interferes the quantification (see Figure S8, Supporting Information). ^jJRC-TIO-4 equivalent to P25. ^kA mixture of P25_anatase and P25_rutile particles with the different ratios (5 mg; A/R = 80/20, 90/10, and 70/30 w/w) was added to the solution. ^lA mixture of JRC-TIO-1 (4 mg) and JRC-TIO-6 particles (1 mg) was added to the solution.

photoirradiation ($\lambda > 300$ nm). Our hypothesis is as follows: (i) photoactivated TiO₂ promotes oxidation of alcohols (aldehydes formation) and reduction of nitroaromatics (anilines formation) by photocatalysis; (ii) Lewis acid sites on the TiO₂ surface^{19,20} promote catalytic condensation of the formed aldehydes with anilines (imine formation). The photocatalytic and catalytic actions occurring on TiO₂ successfully promote one-pot imine synthesis without noble metals at room temperature.

TiO₂ has two common polymorphic forms: anatase and rutile, and a mixture of anatase and rutile particles (ca. 80/20 w/w) has widely been used for photocatalysis, available as AEROXIDE P25 TiO₂ by Degussa (Evonik).²¹ Here we report that photoirradiation ($\lambda > 300$ nm) of P25 TiO₂ in alcohol containing nitrobenzene at room temperature successfully promotes one-pot synthesis of imines with very high yields (90%). Other commercially available anatase or rutile TiO₂ particles, however, exhibit very low yields (<30%). To clarify the high activity of P25 TiO₂, anatase and rutile particles were isolated from P25 TiO₂ by chemical treatments. Photocatalysis experiments revealed that the active sites for photocatalytic oxidation of alcohols and reduction of nitroaromatics on P25 TiO₂ are the rutile particles. In contrast, catalysis experiments revealed that the anatase particles isolated from P25 TiO₂ exhibit very high activity for catalytic condensation of the formed aldehyde and aniline due to the large number of Lewis acid sites. The P25 TiO₂ particles therefore successfully promote the tandem photocatalytic and catalytic reactions on

the respective rutile and anatase particles, thus producing imines with very high yields.

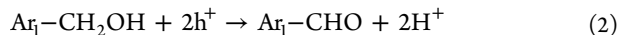
RESULTS AND DISCUSSION

Catalytic Activity. Synthesis of *N*-benzylidenaniline (**1**) from benzyl alcohol and nitrobenzene was carried out using various kinds of TiO₂ particles with different crystalline phases, particle sizes, and Brunauer–Emmett–Teller (BET) surface areas. Table 1 summarizes the results of photoirradiation ($\lambda > 300$ nm) of TiO₂ (5 mg) in benzyl alcohol (5 mL) with nitrobenzene (50 μmol) under N₂ atmosphere (1 atm) for 10 h. With anatase TiO₂ (samples 1–3), the imine yields are very low (<28%), and the nitrobenzene conversions are also insufficient (<63%). This indicates that anatase TiO₂ are not active for nitrobenzene reduction and result in low imine yields. In contrast, rutile TiO₂ (samples 4–6) consumes almost all of nitrobenzene (>99%), but their imine yields are very low (<24%). This means that, on rutile TiO₂, condensation of aldehyde with aniline does not occur efficiently. However, as shown by the sample 7, P25 TiO₂ promotes complete disappearance of nitrobenzene (>99%) and produces imine with very high yield (90%), suggesting that P25 TiO₂ specifically promotes efficient and selective imine formation. In addition, the P25 TiO₂ catalyst recovered after the reaction, when reused for further reaction, exhibits almost the same imine yields as the fresh catalyst. This indicates that the catalyst is stable even under UV irradiation and reusable without loss of activity and selectivity.

Mechanism for Imine Formation. The imine formation is promoted by tandem photocatalytic and catalytic actions of TiO_2 , as follows. The reaction is initiated by photoexcitation of TiO_2 , producing positive hole (h^+) and conduction band electron (e^-) pairs.



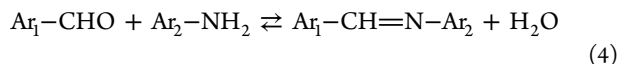
The h^+ oxidize alcohols and produce aldehydes and protons.



The e^- reduce nitroaromatics and produce anilines.



Condensation of the formed aldehydes and anilines catalyzed by the Lewis acid sites on the TiO_2 surface^{19,20} produces imines.



As a result of this, the entire reaction can be written as eq 5; the reaction of nitroaromatics with three equivalents of alcohols gives rise to imine with two equivalents of aldehydes and three equivalents of water.

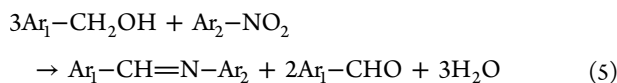


Figure 1 summarizes the time-dependent change in the amounts of substrate and products during the reaction of

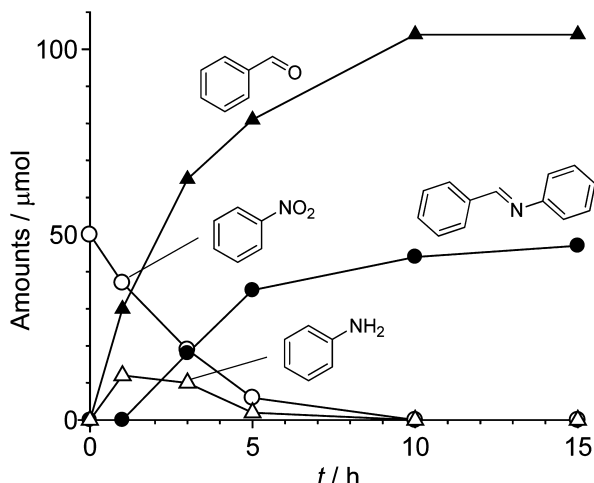


Figure 1. Time-dependent change in the amounts of substrate and products during the reaction of benzyl alcohol and nitrobenzene with P25 TiO_2 (sample 7) under photoirradiation. The reaction conditions are identical to those in Table 1.

benzyl alcohol and nitrobenzene with P25 TiO_2 (sample 7) under photoirradiation. At the early stage of reaction, benzaldehyde and aniline are produced, along with a decrease in the amount of nitrobenzene. The amount of aniline decreases with time, along with imine formation. After 10 h of irradiation, almost all of the substrate nitrobenzene is transformed to imine (90%), with the formation of almost 2 equiv of benzaldehyde. This is fully consistent with eq 5. The results clearly suggest that the above reaction sequence (eqs 1–4) consisting of photocatalytic and catalytic reactions indeed proceeds on the P25 TiO_2 catalyst. Figure S1 (Supporting

Information) shows the time-dependent changes in the amounts of substrate and products on other commercially available anatase (JRC-TIO-1; sample 1) and rutile TiO_2 (JRC-TIO-6; sample 6). The anatase TiO_2 shows very low activity for nitrobenzene reduction. The rutile TiO_2 is successful for nitrobenzene reduction but unsuccessful for condensation of aldehyde and aniline. These data suggest that P25 TiO_2 specifically promotes the above reaction sequence (eqs 1–4) very efficiently.

Isolation of Anatase and Rutile Particles from P25

TiO_2 . As shown in Table 1, anatase or rutile particles alone are ineffective for imine formation, whereas P25 TiO_2 , a mixture of anatase and rutile particles, produces imine with very high yield. The reason for high activity of P25 TiO_2 must therefore be clarified. We isolated respective anatase and rutile particles from P25 TiO_2 by chemical treatments and studied their photocatalytic and catalytic properties. As reported,²² rutile particles are dissolved into a mixture of H_2O_2 and NH_3 more easily than anatase; therefore, anatase particles can be isolated from P25 TiO_2 by simple washing treatment. P25 TiO_2 (6 g) was added to a H_2O_2 solution (30 wt %, 200 mL) mixed with an NH_3 solution (25 wt %, 6 mL), and stirred for 15 h at 298 K. The resultant was thoroughly washed with water, freeze-dried, and calcined in air at 473 K for 2.5 h, affording white powders of anatase particles (P25_anatase). In contrast, as reported,²³ a hydrofluoric acid (HF) solution dissolves anatase particles more easily than rutile; therefore, rutile particles can be isolated from P25 TiO_2 . P25 particles (1 g) were stirred in an HF solution (10 wt %, 50 mL) for 24 h at 298 K. The resultant was thoroughly washed with water until the pH of solution becomes ca. 7 and dried in vacuo for 12 h, affording white powders of rutile particles (P25_rutile).

Figure 2 shows the X-ray diffraction (XRD) patterns of respective particles. P25 TiO_2 exhibits diffractions for both anatase and rutile crystallites. As shown in Table 1 (sample 7), the ratio of respective crystallites was determined based on the

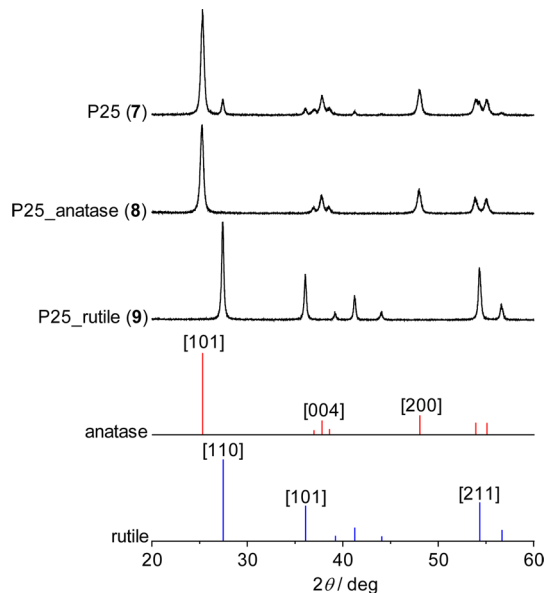


Figure 2. XRD patterns of respective TiO_2 particles and standard patterns for anatase (JCPDS 21-1272) and rutile (JCPDS 21-1276). The texts in the parentheses denote the sample numbers listed in Table 1. The patterns for other TiO_2 are summarized in Figure S2 (Supporting Information).

ratio of their intensities to be 83:17.²⁴ In contrast, the isolated P25_anatase or P25_rutile particles respectively show anatase or rutile diffractions. Figure 3 shows the diffuse reflectance

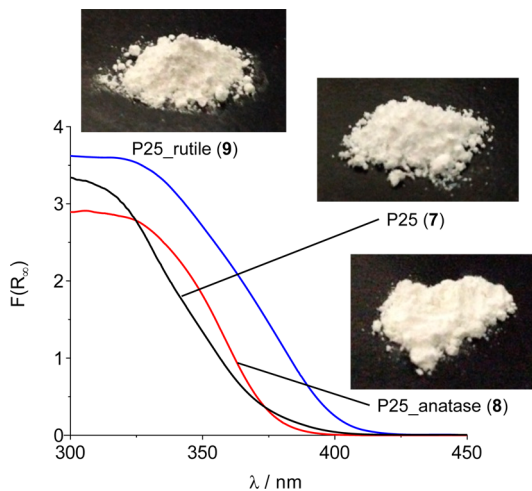


Figure 3. Diffuse reflectance UV–vis spectra of respective TiO_2 . The spectra for other catalysts are summarized in Figure S3 (Supporting Information).

UV–vis spectra of the particles. The absorption edge of P25 TiO_2 is ca. 410 nm. P25_anatase and P25_rutile particles, however, show blue-shifted and red-shifted band, respectively, which are similar to those of other anatase and rutile particles (Figure S3, Supporting Information).²⁵ These data suggest that anatase and rutile particles are successfully isolated from P25 TiO_2 by the $\text{H}_2\text{O}_2/\text{NH}_3$ and HF treatments.

Figure 4 shows the typical transmission electron microscopy (TEM) images of respective particles. As shown in Figure 4a, P25 TiO_2 is a mixture of small particles (20–40 nm diameters) and large particles (60–100 nm diameters), which are assigned to anatase and rutile particles, respectively.²³ As shown in Figure 4b and c, P25_anatase particles consist of small particles with 20–40 nm diameters, and P25_rutile particles consist of large particles with >50 nm diameters. Figure 5 shows the size distribution of the respective particles determined by dynamic laser scattering (DLS) analysis. As shown by the black line, P25 TiO_2 exhibits bimodal particle size distribution with average diameters 27 and 340 nm, respectively.²⁶ The smaller particles are assigned to the dispersed anatase particles,²⁷ and the larger ones are assigned to the interwoven aggregates of anatase and rutile particles.²⁸ As shown by the red line, P25_anatase particles show monodispersed distribution with average diameter 27 nm. In contrast, P25_rutile particles (blue line) show monodispersed distribution with average diameter 71 nm. These distributions are fully consistent with the TEM observations (Figure 4). The above XRD, UV–vis, TEM, and DLS analyses clearly suggest that the $\text{H}_2\text{O}_2/\text{NH}_3$ and HF treatments of P25 TiO_2 particles successfully isolate the anatase and rutile particles.

The $\text{H}_2\text{O}_2/\text{NH}_3$ and HF treatments of P25 TiO_2 scarcely affect the surface morphology of the isolated anatase and rutile particles. XPS, IR, and Zeta potential analysis confirm this. As shown in Figure S5 (Supporting Information), XPS charts of isolated P25_anatase and P25_rutile particles do not show N 1s²⁹ and F 1s³⁰ peaks at around 400 and 690 eV, respectively (detection limit: ca. 0.1 atom %).³¹ This suggests that these isolated particles scarcely contain N and F atoms even after

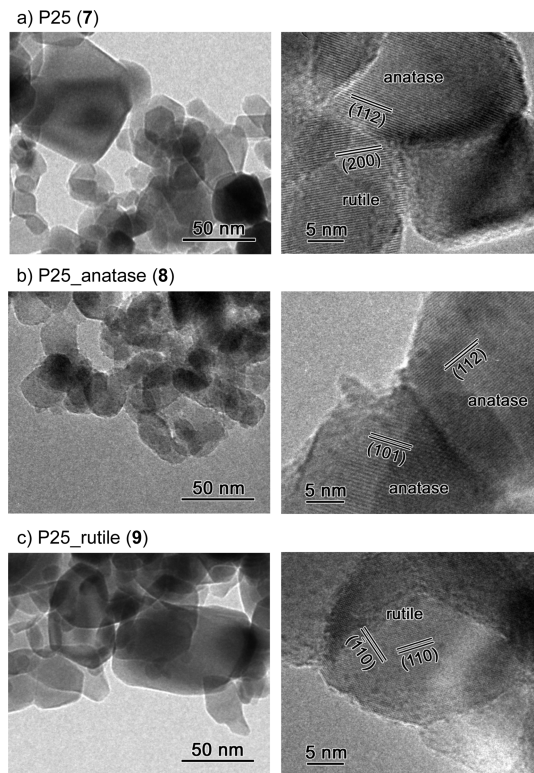


Figure 4. Typical (left) TEM and (right) high-resolution TEM images of (a) P25, (b) P25_anatase, and (c) P25_rutile particles, respectively.

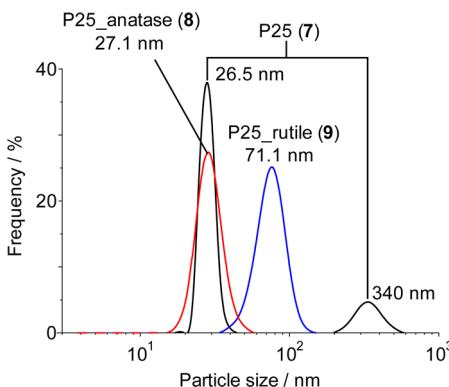


Figure 5. Size distribution of TiO_2 particles determined by DLS analysis. The distributions of other TiO_2 particles are summarized in Figure S4 (Supporting Information).

$\text{H}_2\text{O}_2/\text{NH}_3$ and HF treatments. Figure S6 (Supporting Information) shows the IR spectra of respective particles measured on KBr disks. Both P25_anatase and P25_rutile particles exhibit a distinctive absorption at ca. 3400 cm^{-1} , assigned to O–H stretching vibration,³² similar to that of P25. In addition, a mixture of these anatase and rutile particles (4/1 wt/wt) shows almost the same spectrum as P25 consisting of 83% anatase and 17% rutile particles. These data suggest that the numbers of surface –OH groups on the particles are scarcely changed even by chemical treatments. Almost no change in the surface properties by the treatments is further supported by zeta potential analysis. As shown in Figure S7 (Supporting Information), potentials of zero charge (PZC) of P25_anatase and P25_rutile particles are 5.8 and 6.0, respectively and are similar to that of P25 (6.0).³³ The above findings clearly suggest that the $\text{H}_2\text{O}_2/\text{NH}_3$ and HF treatments

of P25 TiO₂ successfully isolate the anatase and rutile particles without change in the surface properties.

The isolated P25_anatase and P25_rutile particles were then used for one-pot imine synthesis from benzyl alcohol and nitrobenzene under photoirradiation. As shown in Table 1 (samples 8 and 9), the imine yields obtained by the respective particles (<56%) are much lower than those of P25 TiO₂ (sample 7). In contrast, as shown by the sample 10, a mixture of P25_anatase (4 mg) and P25_rutile (1 mg), when used for the reaction, exhibits very high activity similar to that obtained with P25 TiO₂ consisting of 83% anatase and 17% rutile particles (5 mg, sample 7). These findings clearly suggest that neither anatase nor rutile particles in P25 TiO₂ are active for one-pot imine synthesis by themselves; combination of these particles promotes tandem photocatalytic and catalytic reactions, facilitating efficient imine production.

Photocatalysis Experiment. To clarify the role of anatase and rutile particles in the efficient imine formation on P25 TiO₂, photocatalytic and catalytic behaviors of the respective particles were studied. Photocatalytic activity was studied first based on the photocatalytic reduction of nitrobenzene to aniline. In that, 2-PrOH, a secondary alcohol, was used in place of benzyl alcohol because the formed acetone does not undergo condensation with the formed aniline.³⁴ Figure 6 summarizes

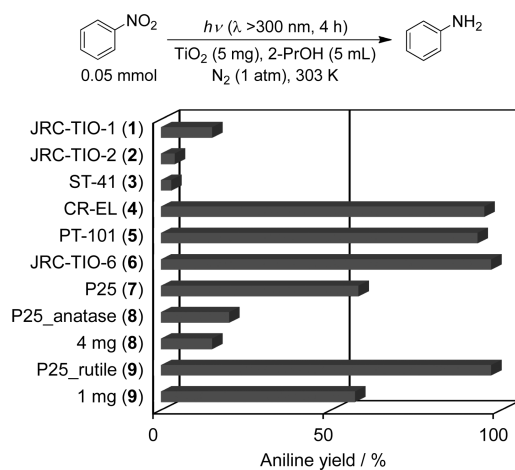


Figure 6. Aniline yields on respective TiO₂ particles during photocatalytic reduction of nitrobenzene in 2-PrOH.

the yields of aniline obtained by photoirradiation of respective TiO₂ particles in 2-PrOH containing nitrobenzene for 4 h. The data for commercially available TiO₂ clearly reveal that anatase TiO₂ (samples 1–3) exhibit very low aniline yields (<15%), but rutile TiO₂ (samples 4–6) show much higher yields (>93%). The higher activity of rutile particles is because, as reported by our previous work,²⁶ they contain a larger number of surface defects, active sites for photocatalytic reduction of nitroaromatics. As shown in Scheme 1a (bottom), the rutile (110) surface is characterized by alternate rows of 5-fold coordinated Ti⁴⁺ atoms (black) and bridging O²⁻ atoms (light green) that run in the [001] direction.³⁵ Surface defects are the O²⁻ vacancies, where two excess electrons associated with O²⁻ are transferred to the empty 3d orbitals of neighboring Ti⁴⁺ atoms, producing two exposed Ti³⁺ atoms.³⁶ As shown in Scheme 1a (top), these Ti³⁺ atoms act as adsorption sites for nitroaromatics³⁴ and trapping sites for conduction band e⁻.³⁷ This

thus results in efficient photocatalytic reduction of nitroaromatics to anilines on the rutile particles.

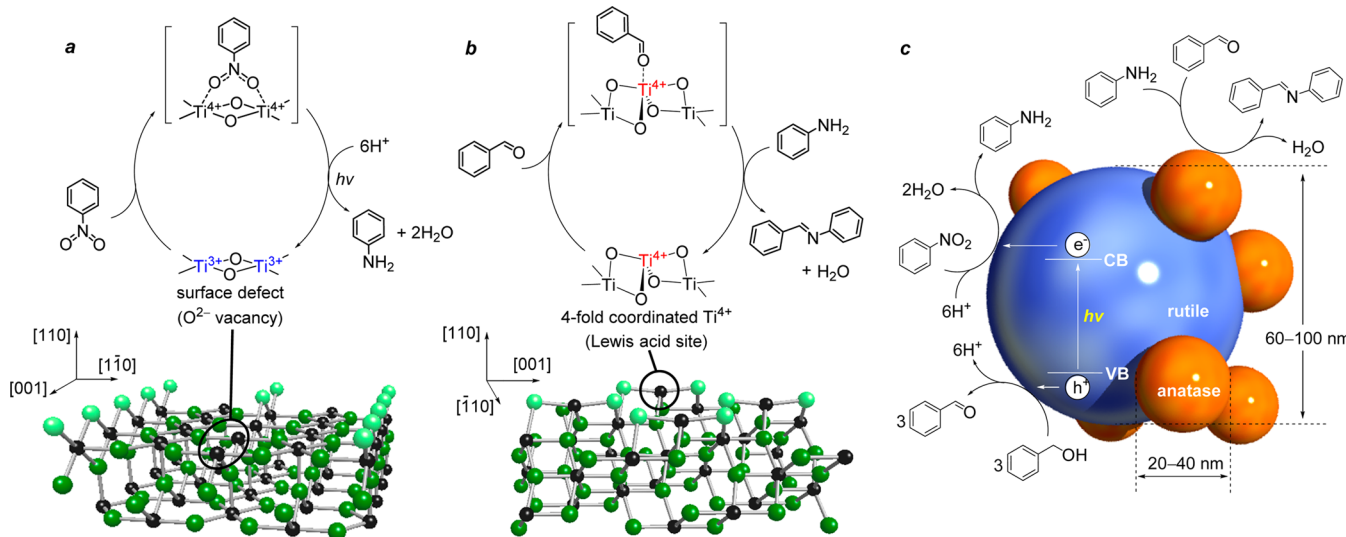
As shown in Figure 6, P25_rutile particles (sample 9) exhibit very high activity for photocatalytic reduction of nitrobenzene, as is the case for other rutile particles (samples 4–6), and the activity is much higher than P25_anatase (sample 8). As summarized in Table 1, P25 TiO₂ consists of 83% anatase and 17% rutile particles. The P25_rutile particles (sample 9, 1 mg), when used for photocatalytic reduction of nitrobenzene (Figure 6), produce aniline with 57% yield. This is similar to that obtained with P25 TiO₂ (sample 7, 5 mg)^{38–41} and is much higher than that obtained with 4 mg P25_anatase (sample 8, 15%). These results clearly suggest that, as shown in Scheme 1a, photocatalytic reduction of nitrobenzene (aniline formation) and oxidation of alcohol (aldehyde formation) on P25 TiO₂ occur predominantly on the rutile particles.

Catalysis Experiment. Catalytic activity for condensation of the formed benzaldehyde and aniline was then studied with respective TiO₂ particles in the dark condition. Benzaldehyde (75 μmol) and aniline (50 μmol) were stirred in benzyl alcohol (5 mL) with respective particles (5 mg) at 298 K in the dark for 3 h under N₂. Figure 7 summarizes the yields of imine 1. P25 TiO₂ (sample 7) exhibits significantly higher activity for condensation compared to other commercially available TiO₂ particles (samples 1–6). P25_rutile particles (sample 9) show much lower activity, but the activity of P25_anatase (sample 8) is comparable to that of P25 TiO₂. This clearly indicates that anatase particles contained in P25 TiO₂ promote efficient condensation of aldehydes and anilines.

It is well-known that Lewis acid sites behave as active sites for dehydration coupling.^{42,43} The number of Lewis acid sites on the respective TiO₂ particles was therefore determined by the pyridine adsorption experiments based on the diffuse-reflectance infrared Fourier transform (DRIFT) analysis.^{44,45} Respective TiO₂ particles (5 mg) were mixed with KBr (45 mg) and placed in a DR cell. The cell was evacuated (0.9 Pa) at 423 K for 3 h. After cooling the cell to 303 K, an excess amount of pyridine (21 μmol) was introduced to the cell at 303 K and left for 1 h. The cell was then evacuated (0.9 Pa) for 1 h to remove the physically adsorbed pyridine. Figure 8 shows the DRIFT spectra obtained on the respective TiO₂ particles. A distinctive absorption appears at 1445 cm⁻¹, which is assigned to the C–N–C stretching vibration (ν_{pyridine}) of the pyridine adsorbed onto the Lewis acid sites.⁴⁶ P25 TiO₂ particles (sample 7) show a band stronger than other commercially available TiO₂ (samples 1–5). P25_rutile particles (sample 9) show very weak band, but P25_anatase particles (sample 8) exhibit very strong band. This suggests that P25_anatase particles contain very large amount of Lewis acid sites.

The number of Lewis acid sites per gram TiO₂ particles ($N_{\text{LA}}/\mu\text{mol g}^{-1}$) can be determined by the amount of the pyridine adsorbed.⁴⁵ The N_{LA} values for respective particles are summarized in Table 1. Figure 9 plots the imine 1 yields obtained by the condensation of benzaldehyde and aniline in the dark condition (Figure 7) with the N_{LA} values for respective TiO₂ particles. A clear relationship is observed although the morphologies (crystalline phase and surface area) of the catalysts are different. This indicates that Lewis acid sites indeed behave as the active sites for catalytic condensation. The N_{LA} value for P25 TiO₂ (48 μmol g⁻¹; sample 7) is much higher than that of other anatase or rutile particles (<15 μmol g⁻¹; samples 1–6). The N_{LA} value for P25_rutile (sample 9) is very low (3 μmol g⁻¹), but that for P25_anatase (sample 8) is

Scheme 1. Catalytic Cycles for (a) Hydrogenation of Nitroaromatics on the Photoactivated Rutile (110) Surface and (b) Condensation of Aldehyde and Aniline on the Lewis Acid Sites of Anatase (110) Surface and (c) Proposed Pathways for the Imine Formation on P25 TiO₂^a



^aThe green, black, and light green spheres represent O, Ti, and 2-fold coordinated O²⁻ atoms, respectively.

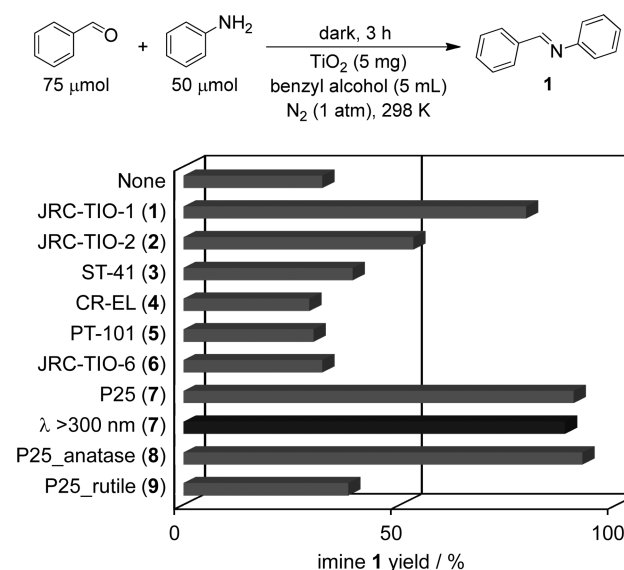


Figure 7. Imine (1) yields obtained during the condensation of benzaldehyde with aniline in the presence of respective TiO₂. The black bar shows the data obtained under UV irradiation ($\lambda > 300$ nm).

significantly higher ($73 \mu\text{mol g}^{-1}$).^{47–51} This suggests that almost all of the Lewis acid sites on P25 TiO₂ exist on the anatase particles, and the high catalytic activity of P25 TiO₂ for condensation is ascribed specifically to the large number of Lewis acid sites on the anatase particles.

During the one-pot imine synthesis in the present system, photocatalytic and catalytic reactions occur simultaneously. The photocatalytic reaction, however, scarcely affects the activity of Lewis acid sites. To clarify this, condensation of benzaldehyde and aniline with P25 TiO₂ (sample 7) was performed under UV irradiation ($\lambda > 300$ nm). As shown in Figure 7 (black bar), the activity is very similar to that obtained in the dark condition. This clearly suggests that photocatalysis occurring on P25 TiO₂ scarcely affects the Lewis acid activity.

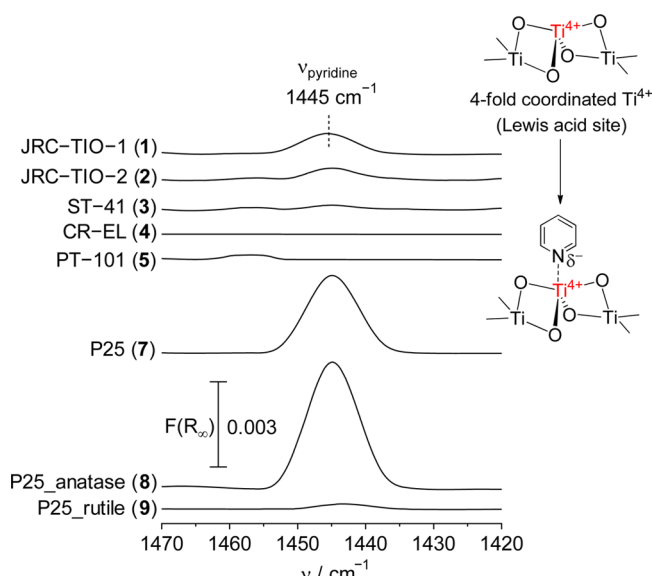


Figure 8. DRIFT spectra of pyridine adsorbed onto the respective TiO₂ particles in the gas phase at 303 K.

Some literature works^{44,52} report that, as shown in Scheme 1b, Lewis acid sites on anatase particles are the *4-fold coordinated Ti⁴⁺* atoms located at the (110) surface.^{53,54} These Ti⁴⁺ atoms accept the electrons of aldehyde oxygen, and subsequent attacking of aniline to the aldehyde produces imine.⁵⁵ Large number of Lewis acid sites on P25 anatase particles (sample 8, Figure 8) therefore implies that they may contain a large amount of anatase (110) surface. However, as reported,⁵⁶ anatase (110) surface cannot be detected by diffraction analysis because of the extinction rule. Recently, some literature works^{57,58} have reported that DRIFT analysis (100 K) of carbon monoxide (CO) adsorbed onto the surface of TiO₂ detected a peak at 2183 cm^{-1} , assigned to the CO adsorbed onto the 4-fold coordinated Ti⁴⁺ atoms. In that, P25 TiO₂ showed the peak much stronger than other commercially

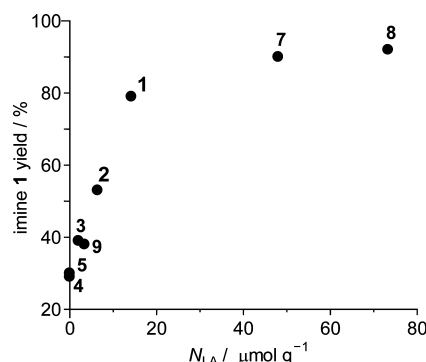


Figure 9. Relationship between the number of Lewis acid sites per gram TiO_2 particles (N_{LA}) and the yield of imine 1 during the condensation of benzaldehyde and aniline on respective TiO_2 in the dark condition (Figure 7).

available TiO_2 ,⁵⁷ although quantitative determination of the Ti^{4+} atoms was not made. These data suggest that P25_anatase particles contain very large amount of (110) surface possessing 4-fold coordinated Ti^{4+} atoms. They behave as Lewis acid sites and result in very high activity for condensation of aldehyde and aniline.

The significantly large amount of (110) surface on the P25_anatase particles probably originates from the synthesis method of P25 TiO_2 . It is well-known that P25 TiO_2 is synthesized by a “dry process” (flame pyrolysis of gaseous TiCl_4).⁵⁹ In contrast, many other commercially available TiO_2 are synthesized by a “wet process” (hydrolysis of Ti precursors followed by calcination).⁶⁰ The dry process may create a large amount of anatase (110) phases on P25 TiO_2 , although it is unclear yet how the (110) phases are specifically created by this process. Nevertheless, the large amount of anatase (110) phase

created on P25 TiO_2 facilitates high activity for catalytic condensation of aldehyde and aniline.

One-Pot Imine Formation on Photoactivated P25 TiO_2

The above findings suggest that the catalytic mechanism for efficient one-pot imine formation on P25 TiO_2 under UV irradiation can be explained as Scheme 1c. The rutile particles of P25 TiO_2 efficiently promote photocatalytic oxidation of alcohols and reduction of nitroaromatics (formation of aldehyde and aniline) on the surface defects (5-fold coordinated Ti^{3+} atoms). In contrast, the anatase particles of P25 TiO_2 catalyze the condensation of the formed aldehyde and aniline (imine formation) because they contain a large amount of 4-fold coordinated Ti^{4+} atoms behaving as active sites for condensation. Combination of these actions on the respective rutile and anatase particles therefore specifically promotes efficient one-pot formation of imines on P25 TiO_2 .

Composition of anatase (83%) and rutile (17%) particles in P25 TiO_2 is very important for efficient one-pot imine synthesis. The respective P25_anatase and P25_rutile particles were mixed with different ratios and used for photocatalytic reaction of benzyl alcohol and nitrobenzene. As shown by the sample 10 in Table 1, the 80/20 w/w mixture, which has a similar composition to P25 (83/17), shows the almost the same activity as that of P25 (sample 7). In contrast, as shown by the samples 11 and 12, the 90/10 and 70/30 w/w mixtures show decreased imine yields. The lower yield on the 90/10 mixture is due to the lower activity for nitrobenzene reduction on small amount of rutile particles. In contrast, the lower yield on the 70/30 mixture is due to the lower activity for condensation on small amount of anatase particles. These data suggest that P25 TiO_2 has the best anatase and rutile composition (83/17 w/w) for efficient one-pot imine formation.

It must also be noted that a mixture of other commercially available anatase and rutile particles also promotes one-pot imine synthesis efficiently. As shown in Table 1 (sample 13),

Table 2. One-Pot Synthesis of Imines from Alcohols and Nitroaromatics on P25 TiO_2 (Sample 7) under Photoirradiation^a

entry	alcohol	nitroarene	t / h	nitroarene conv. /% ^b	product	yield / % ^b
1			10	>99		90
2			12	>99		80
3			12	>99		96
4			12	>99		88
5			15	>99		82
6 ^{c,d}			12	>99		82
7 ^{c,d}			12	>99		83
8 ^{c,e}			18	>99		80

^aReaction conditions: catalyst (5 mg), alcohol (5 mL), nitroarene (50 μmol), temperature (298 K), N_2 (1 atm), Xe lamp ($\lambda > 300$ nm).

^bDetermined by GC analysis. ^c CH_2Cl_2 solution (5 mL) containing an alcohol (10 wt %) was used as solvent to fully dissolve the products. ^dCatalyst (20 mg). ^eCatalyst (50 mg).

the reaction with a 80/20 w/w mixture of anatase (JRC-TIO-1, sample 1) and rutile (JRC-TIO-6, sample 6) produces the corresponding imine with high yield (89%), although the use of sample 1 or 6 alone produces the imine with only 18 or 5% yield. The high imine yield (89%) indicates that a mixture of other commercially available anatase and rutile particles also behaves as the catalyst for efficient one-pot imine synthesis as well as P25 TiO₂.

The P25 TiO₂ catalyst is applicable to the synthesis of several kinds of substituted aromatic imines. As summarized in Table 2, photoirradiation of P25 TiO₂ with substituted benzyl alcohols and/or nitroaromatics successfully produces the corresponding imines with very high yields (>80%). In particular, reducible substituents such as halogen and vinyl groups on the alcohols and nitroarenes are retained unchanged during photoreaction (entries 4–7). These data suggest that P25 TiO₂ promotes chemoselective reduction of nitroaromatics and successfully produces substituted imines.

CONCLUSION

We found that P25 TiO₂, a mixture of anatase and rutile particles (ca. 80/20 w/w), successfully promotes one-pot imine synthesis from alcohol and nitroaromatics under UV irradiation. The rutile particles of P25 TiO₂ behave as photocatalytic active site for oxidation of alcohols (aldehyde formation) and reduction of nitroaromatics (aniline formation). In contrast, the anatase particles in P25 TiO₂ act as catalytic site for condensation of the formed aldehydes and anilines (imines formation). The photocatalytic and catalytic actions on the respective particles therefore facilitate tandem reactions, producing imines with very high yields. The P25 TiO₂ system has several advantages over early reported systems for imine synthesis: (i) stable substrates (alcohols and nitroaromatics); (ii) noble-metal-free catalyst (TiO₂); and (iii) mild reaction conditions (room temperature). The system therefore shows potential for green imine synthesis. The results presented here based on the tandem photocatalytic and catalytic actions on P25 TiO₂ may contribute to the design of more efficient catalytic systems for imine synthesis and may help open a new strategy toward green organic synthesis based on photocatalysis.

EXPERIMENTAL SECTION

Materials. All of the reagents were purchased from Wako, Tokyo Kasei, and Sigma-Aldrich and used without further purification. Water was purified by the Milli Q system. P25_anatase particles were isolated by stirring P25 particles (6 g) in an H₂O₂ solution (30 wt %, 200 mL) with an NH₃ solution (25 wt %, 6 mL) at 298 K for 15 h. After centrifugation, the collected powders were washed with water, freeze-dried, and calcined in air at 473 K for 2.5 h. Care must be taken to avoid explosive reaction (see the Supporting Information). P25_rutile particles were isolated as follows: P25 particles (1 g) were stirred in an HF solution (10 wt %, 50 mL) for 24 h at 298 K. The resultant was washed thoroughly with water until the pH of the solution becomes about 7 and dried in vacuo for 12 h.

Photoreaction Procedure. Each nitroarene was dissolved in an alcohol solution (5 mL). The solution and catalyst were added to a Pyrex glass tube (φ 12 mm; capacity, 20 mL), and the tube was sealed with a rubber septum cap. The catalyst was dispersed well by ultrasonication for 5 min, and N₂ was bubbled through the solution for 5 min. The tube was immersed in a water bath controlled at 298 K (error: ± 0.5 K)⁶¹ and photoirradiated with magnetic stirring using a 2 kW Xe lamp (USHIO Inc.; $\lambda > 300$ nm).⁶² After the reaction, the catalyst was recovered by centrifugation, and the resulting solution was analyzed by GC-FID. The substrate and product concentrations were

calibrated with authentic samples. Analysis was performed at least three times, and the errors were $\pm 0.2\%$.

Analysis. XRD patterns were measured on a Philips X'Pert-MPD spectrometer.²⁶ TEM observations were carried out using a FEI Tecnai G2 20ST analytical electron microscope operated at 200 kV.⁶³ DLS analysis was performed on a Horiba LB-500 dynamic light-scattering particle size analyzer.⁶⁴ DRIFT analysis was carried out on a FTIR 610 system equipped with a DR-600B in situ cell (JASCO Corp.).⁶⁵ DR UV-vis spectra were measured on an UV-vis spectrophotometer (JASCO Corp.; V-550 equipped with Integrated Sphere Apparatus ISV-469) with BaSO₄ as a reference.⁶⁶ XPS analysis was performed using a JEOL JPS-9000MX spectrometer with Mg K α radiation as the energy source.⁶⁷ Zeta potentials were measured on an ELSZ-1000 analyzer (Otsuka Electronics Co., Ltd.).

ASSOCIATED CONTENT

S Supporting Information

Safer procedure for anatase separation, time-dependent changes in the amounts of substrate and products during the reaction on some TiO₂ (Figure S1), XRD patterns (Figure S2), DR UV-vis spectra (Figure S3), size distribution (Figure S4), XPS charts (Figure S5), IR spectra of TiO₂ (Figure S6), zeta potentials (Figure S7), and DRIFT spectra of pyridine adsorbed onto TiO₂ (Figure S8). This material is available free of charge via the Internet at <http://pubs.acs.org>.

AUTHOR INFORMATION

Corresponding Author

*E-mail: shiraish@cheng.es.osaka-u.ac.jp.

Notes

The authors declare no competing financial interest.

ACKNOWLEDGMENTS

This work was supported by the Grant-in-Aid for Scientific Research (No. 26289296) from the Ministry of Education, Culture, Sports, Science and Technology, Japan (MEXT).

REFERENCES

- Martin, S. F. Recent Applications of Imines as Key Intermediates in the Synthesis of Alkaloids and Novel Nitrogen Heterocycles. *Pure Appl. Chem.* **2009**, *81*, 195–204.
- Tang, W.; Zhang, X. New Chiral Phosphorus Ligands for Enantioselective Hydrogenation. *Chem. Rev.* **2003**, *103*, 3029–3069.
- Layer, R. W. The Chemistry of Imines. *Chem. Rev.* **1963**, *63*, 489–510.
- Adams, J. P. Imines, Enamines and Oximes. *J. Chem. Soc., Perkin Trans. 1* **2000**, 125–139.
- Nicolaou, K. C.; Mathison, C. J. N.; Montagnon, T. New Reactions of IBX: Oxidation of Nitrogen- and Sulfur-Containing Substrates To Afford Useful Synthetic Intermediates. *Angew. Chem., Int. Ed.* **2003**, *42*, 4077–4082.
- Hirano, M.; Yakabe, S.; Chikamori, H.; Clark, J. H.; Morimoto, T. Oxidation by Chemical Manganese Dioxide. Part 3. Oxidation of Benzylidene and Allylic Alcohols, Hydroxyarenes and Aminoarenes. *J. Chem. Res.* **1998**, 770–771.
- Samec, J. S. M.; Ell, A. H.; Bäckvall, J.-E. Efficient Ruthenium-Catalyzed Aerobic Oxidation of Amines by Using a Biomimetic Coupled Catalytic System. *Chem.—Eur. J.* **2005**, *11*, 2327–2334.
- Wang, J.-R.; Fu, Y.; Zhang, B.-B.; Cui, X.; Liu, L.; Guo, Q.-X. Palladium-Catalyzed Aerobic Oxidation of Amines. *Tetrahedron Lett.* **2006**, *47*, 8293–8297.
- Yuan, H.; Yoo, W.-J.; Miyamura, H.; Kobayashi, S. Discovery of a Metalloenzyme-like Cooperative Catalytic System of Metal Nano-clusters and Catechol Derivatives for the Aerobic Oxidation of Amines. *J. Am. Chem. Soc.* **2012**, *134*, 13970–13973.

- (10) Billman, J. H.; Tai, K. M. Reduction of Schiff Bases. II. Benzydrylamines and Structurally Related Compounds. *J. Org. Chem.* **1958**, *23*, 535–539.
- (11) Varma, R. S.; Dahiya, R.; Kumar, S. Clay Catalyzed Synthesis of Imines and Enamines under Solvent-Free Condition Using Microwave Irradiation. *Tetrahedron Lett.* **1997**, *38*, 2039–2042.
- (12) Liu, G.; Cogan, D. A.; Owens, T. D.; Tang, T. P.; Ellman, J. A. Synthesis of Enantiomerically Pure *N*-*tert*-Butanesulfinyl Imines (*tert*-Butanesulfinimines) by the Direct Condensation of *tert*-Butanesulfonamide with Aldehydes and Ketones. *J. Org. Chem.* **1999**, *64*, 1278–1284.
- (13) Liu, Y.; Chen, W.; Feng, C.; Deng, G. Ruthenium-Catalyzed One-Pot Aromatic Secondary Amine Formation from Nitroarenes and Alcohols. *Chem. Asian. J.* **2011**, *6*, 1142–1146.
- (14) Cano, R.; Ramón, D. J.; Yus, M. Impregnated Ruthenium on Magnetite as a Recyclable Catalyst for the N-Alkylation of Amines, Sulfonamides, Sulfinamides, and Nitroarenes Using Alcohols as Electrophiles by a Hydrogen Autotransfer Process. *J. Org. Chem.* **2011**, *76*, 5547–5557.
- (15) Tang, L.; Sun, H.; Li, Y.; Zha, Z.; Wang, Z. Highly Active and Selective Synthesis of Imines from Alcohols and Amines or Nitroarenes Catalyzed by Pd/DNA in Water with Dehydrogenation. *Green Chem.* **2012**, *14*, 3423–3428.
- (16) Cui, X.; Zhang, C.; Shi, F.; Deng, Y. Au/Ag–Mo Nano-Rods Catalyzed Reductive Coupling of Nitrobenzenes and Alcohols Using Glycerol as the Hydrogen Source. *Chem. Commun.* **2012**, *48*, 9391–9393.
- (17) Zanardi, A.; Mata, J. A.; Peris, E. One-Pot Preparation of Imines from Nitroarenes by a Tandem Process with an Ir–Pd Heterodimetallic Catalyst. *Chem.—Eur. J.* **2010**, *16*, 10502–10506.
- (18) Sabater, S.; Mata, J. A.; Paris, E. Dual Catalysis with an Ir^{III}–Au^I Heterodimetallic Complex: Reduction of Nitroarenes by Transfer Hydrogenation using Primary Alcohols. *Chem.—Eur. J.* **2012**, *18*, 6380–6385.
- (19) Hakki, A.; Dillert, R.; Bahnemann, D. W. Factors Affecting the Selectivity of the Photocatalytic Conversion of Nitroaromatic Compounds over TiO₂ to Valuable Nitrogen-Containing Organic Compounds. *Phys. Chem. Chem. Phys.* **2013**, *15*, 2992–3002.
- (20) Shiraishi, Y.; Fujiwara, K.; Sugano, Y.; Ichikawa, S.; Hirai, T. N-Monoalkylation of Amines with Alcohols by Tandem Photocatalytic and Catalytic Reactions on TiO₂ Loaded with Pd Nanoparticles. *ACS Catal.* **2013**, *3*, 312–320.
- (21) Ohtani, B.; Prieto-Mahaney, O. O.; Li, D.; Abe, R. What is Degussa (Evonik) P25? Crystalline Composition Analysis, Reconstruction from Isolated Pure Particles and Photocatalytic Activity Test. *J. Photochem. Photobiol., A* **2010**, *216*, 179–182.
- (22) Ohtani, B.; Azuma, Y.; Li, D.; Ihara, T.; Abe, R. Isolation of Anatase Crystallites from Anatase–Rutile Mixed Particles by Dissolution with Aqueous Hydrogen Peroxide and Ammonia. *Trans. Mater. Res. Soc. Jpn.* **2007**, *32*, 401–404.
- (23) Ohno, T.; Sarukawa, K.; Matsumura, M. Photocatalytic Activities of Pure Rutile Particles Isolated from TiO₂ Powder by Dissolving the Anatase Component in HF Solution. *J. Phys. Chem. B* **2001**, *105*, 2417–2420.
- (24) Ramis, G.; Busca, G.; Cristiani, C.; Lietti, L.; Forzatti, P.; Bregani, F. Characterization of Tungsta-Titania Catalysts. *Langmuir* **1992**, *8*, 1744–1749.
- (25) Zhang, Q.; Gao, L.; Guo, J. Effects of Calcination on the Photocatalytic Properties of Nanosized TiO₂ Powders Prepared by TiCl₄ Hydrolysis. *Appl. Catal., B* **2000**, *26*, 207–215.
- (26) Shiraishi, Y.; Hirakawa, H.; Togawa, Y.; Sugano, Y.; Ichikawa, S.; Hirai, T. Rutile Crystallites Isolated from Degussa (Evonik) P25 TiO₂: Highly Efficient Photocatalyst for Chemoselective Hydrogenation of Nitroaromatics. *ACS Catal.* **2013**, *3*, 2318–2326.
- (27) Ohno, T.; Sarukawa, K.; Tokieda, K.; Matsumura, M. Morphology of a TiO₂ Photocatalyst (Degussa, P-25) Consisting of Anatase and Rutile Crystalline Phases. *J. Catal.* **2001**, *203*, 82–86.
- (28) Bickley, R. I.; Gonzalez-carreno, T.; Lees, J. S.; Palmisano, L.; Tilley, R. J. D. A Structural Investigation of Titanium Dioxide Photocatalysts. *J. Solid State Chem.* **1991**, *92*, 178–190.
- (29) Asahi, R.; Morikawa, T.; Ohwaki, T.; Aoki, K.; Tada, Y. Visible-Light Photocatalysis in Nitrogen-Doped Titanium Oxides. *Science* **2001**, *293*, 269–271.
- (30) Yu, J. C.; Yu, J.; Ho, W.; Jiang, Z.; Zhang, L. Effects of F[−] Doping on the Photocatalytic Activity and Microstructures of Nanocrystalline TiO₂ Powders. *Chem. Mater.* **2002**, *14*, 3808–3816.
- (31) Behner, H.; Gieres, G.; Sipos, B. Characterization of Sputter-Deposited YBaCuO Films by X-ray Photoelectron Spectroscopy. *Fresen. J. Anal. Chem.* **1991**, *341*, 301–307.
- (32) Chen, X.; Wang, X.; Hou, Y.; Huang, J.; Wu, L.; Fu, X. The Effect of Postnitridation Annealing on the Surface Property and Photocatalytic Performance of N-doped TiO₂ under Visible Light Irradiation. *J. Catal.* **2008**, *255*, 59–67.
- (33) Bourikas, K.; Hiemstra, T.; Van Riemsdijk, W. H. Ion Pair Formation and Primary Charging Behavior of Titanium Oxide (Anatase and Rutile). *Langmuir* **2001**, *17*, 749–756.
- (34) Shiraishi, Y.; Togawa, Y.; Tsukamoto, D.; Tanaka, S.; Hirai, T. Highly Efficient and Selective Hydrogenation of Nitroaromatics on Photoactivated Rutile Titanium Dioxide. *ACS Catal.* **2012**, *2*, 2475–2481.
- (35) Papageorgiou, A. C.; Beglitis, N. S.; Pang, C. L.; Teobaldi, G.; Cabailh, G.; Chen, Q.; Fisher, A. J.; Hofer, W. A.; Thornton, G. Electron Traps and Their Effect on the Surface Chemistry of TiO₂ (110). *Proc. Natl. Acad. Sci. U.S.A.* **2010**, *107*, 2391–2396.
- (36) Rodriguez, J. A.; Jirsak, T.; Liu, G.; Hrbek, J.; Dvorak, J.; Maiti, A. Chemistry of NO₂ on Oxide Surfaces: Formation of NO₃ on TiO₂ (110) and NO₂↔O Vacancy Interactions. *J. Am. Chem. Soc.* **2001**, *123*, 9597–9605.
- (37) Dohnálek, Z.; Lyubinetsky, I.; Rousseau, R. Thermally-Driven Processes on Rutile TiO₂ (110)-(1×1): A Direct View at the Atomic Scale. *Prog. Surf. Sci.* **2010**, *85*, 161–205.
- (38) As reported in several papers (for example, refs 21 and 39–41), P25 TiO₂ exhibits higher activity for some photocatalytic reactions than anatase or rutile, due to their enhanced charge separation at the anatase/rutile interface. The similar photocatalytic activity of P25_rutile (1 mg) to that of P25 TiO₂ (5 mg) in Figure 6, however, indicates that the charge separation at the anatase/rutile interface of P25 TiO₂ scarcely affects the photocatalytic activity; surface defects on the rutile particles in P25 are the active sites for photocatalysis.
- (39) Kawahara, T.; Konishi, Y.; Tada, H.; Tohge, N.; Nishii, J.; Ito, S. A Patterned TiO₂(Anatase)/TiO₂(Rutile) Bilayer-Type Photocatalyst: Effect of the Anatase/Rutile Junction on the Photocatalytic Activity. *Angew. Chem., Int. Ed.* **2002**, *41*, 2811–2813.
- (40) Miyagi, T.; Kamei, M.; Mitsuhashi, T.; Ishigaki, T.; Yamazaki, A. Charge Separation at the Rutile/Anatase Interface: a Dominant Factor of Photocatalytic Activity. *Chem. Phys. Lett.* **2004**, *390*, 399–402.
- (41) Nakajima, H.; Mori, T.; Shen, Q.; Toyoda, T. Photoluminescence Study of Mixtures of Anatase and Rutile TiO₂ Nanoparticles: Influence of Charge Transfer between the Nanoparticles on Their Photoluminescence Excitation Bands. *Chem. Phys. Lett.* **2005**, *409*, 81–84.
- (42) Di Cosimo, J. I.; Díez, V. K.; Xu, M.; Iglesia, E.; Apesteguía, C. R. A. Structure and Surface and Catalytic Properties of Mg-Al Basic Oxides. *J. Catal.* **1998**, *178*, 499–510.
- (43) Wang, W.; Mei, Y.; Li, H.; Wang, J. A Novel Pyrrolidine Imide Catalyzed Direct Formation of α,β -Unsaturated Ketones from Unmodified Ketones and Aldehydes. *Org. Lett.* **2005**, *7*, 601–604.
- (44) Nakajima, K.; Noma, R.; Kitano, M.; Hara, M. Titania as an Early Transition Metal Oxide with a High Density of Lewis Acid Sites Workable in Water. *J. Phys. Chem. C* **2013**, *117*, 16028–16033.
- (45) Hatayama, F.; Ohno, T. Structure and Acidity of Vanadium Oxide layered on Titania (Anatase and Rutile). *J. Chem. Soc. Faraday Trans.* **1991**, *87*, 2629–2633.
- (46) Green, I. X.; Buda, C.; Zhang, Z.; Neurock, M.; Yates, J. T., Jr. IR Spectroscopic Measurement of Diffusion Kinetics of Chemisorbed

- Pyridine through TiO_2 Particles. *J. Phys. Chem. C* **2010**, *114*, 16649–16659.
- (47) The N_{LA} value for anatase particles isolated from P25 TiO_2 ($73 \mu\text{mol g}^{-1}$) is, however, lower than that of commonly used heterogeneous Lewis acid catalysts such as Nb_2O_5 ($150 \mu\text{mol g}^{-1}$; ref 48), zeolite H-BEA ($150 \mu\text{mol g}^{-1}$; ref 49), mesoporous alminosilicate (270 – $370 \mu\text{mol g}^{-1}$; ref 50), and titanosilicate ETS-10 ($289 \mu\text{mol g}^{-1}$; ref 51).
- (48) Nakajima, K.; Baba, Y.; Noma, R.; Kitano, M.; Kondo, J. N.; Hayashi, S.; Hara, M. $\text{Nb}_2\text{O}_5\text{-nH}_2\text{O}$ as a Heterogeneous Catalyst with Water-Tolerant Lewis Acid Sites. *J. Am. Chem. Soc.* **2011**, *133*, 4224–4227.
- (49) Penzien, J.; Abraham, A.; van Bokhoven, J. A.; Jentys, A.; Müller, T. E.; Sievers, C.; Lercher, J. A. Generation and Characterization of Well-Defined Zn^{2+} Lewis Acid Sites in Ion Exchanged Zeolite BEA. *J. Phys. Chem. B* **2004**, *108*, 4116–4126.
- (50) Occelli, M. L.; Biz, S.; Auoux, A.; Ray, G. J. Effects of the Nature of the Aluminum Source on the Acidic Properties of Some Mesostructured Materials. *Microporous Mesoporous Mater.* **1998**, *26*, 193–213.
- (51) Li, J.; Shen, B.; Guo, Q.; Zhang, W.; Wen, G.; Tian, R.; Zhang, Z. Preparation of the Surface Ti, Al Rich ETS-10 and Modification of Its Pore Structure and Acidity by Desilication and Realumination. *Microporous Mesoporous Mater.* **2011**, *145*, 224–230.
- (52) Busca, G.; Saussey, H.; Saur, O.; Lavalle, J. C.; Lorenzelli, V. FT-IR Characterization of the Surface Acidity of Different Titanium Dioxide Anatase Preparations. *Appl. Catal.* **1985**, *14*, 245–260.
- (53) Arrouvel, C.; Digne, M.; Breyses, M.; Toulhoat, H.; Raybaud, P. Effects of Morphology on Surface Hydroxyl Concentration: a DFT Comparison of Anatase– TiO_2 and γ -Alumina Catalytic Supports. *J. Catal.* **2004**, *222*, 152–166.
- (54) Martsinovich, N.; Troisi, A. How TiO_2 Crystallographic Surfaces Influence Charge Injection Rates from a Chemisorbed Dye Sensitiser. *Phys. Chem. Chem. Phys.* **2012**, *14*, 13392–13401.
- (55) Sithambaram, S.; Kumar, R.; Son, Y.-C.; Suib, S. L. Tandem Catalysis: Direct Catalytic Synthesis of Imines from Alcohols Using Manganese Octahedral Molecular Sieves. *J. Catal.* **2008**, *253*, 269–277.
- (56) Liu, M.; Piao, L.; Zhao, L.; Ju, S.; Yan, Z.; He, T.; Zhou, C.; Wang, W. Anatase TiO_2 Single Crystals with Exposed {001} and {110} Facets: Facile Synthesis and Enhanced Photocatalysis. *Chem. Commun.* **2010**, *46*, 1664–1666.
- (57) Deiana, C.; Minella, M.; Tabacchi, G.; Maurino, V.; Fois, E.; Martra, G. Shape-Controlled TiO_2 Nanoparticles and TiO_2 P25 Interacting with CO and H_2O_2 Molecular Probes: a Synergic Approach for Surface Structure Recognition and Physico-Chemical Understanding. *Phys. Chem. Chem. Phys.* **2013**, *15*, 307–315.
- (58) Deiana, C.; Tabacchi, G.; Maurino, V.; Coluccia, S.; Martra, G.; Fois, E. Surface Features of TiO_2 Nanoparticles: Combination Modes of Adsorbed CO Probe the Stepping of (101) Facets. *Phys. Chem. Chem. Phys.* **2013**, *15*, 13391–13399.
- (59) Sachtleben Chemie GmbH, Duisburg, Germany, June 24, 1994.
- (60) Kirchnerova, J.; Herrera Cohen, M.-L.; Guy, C.; Klvana, D. Photocatalytic Oxidation of *n*-Butanol under Fluorescent Visible Light Lamp over Commercial TiO_2 (Hombicat UV100 and Degussa P25). *Appl. Catal., A* **2005**, *282*, 321–332.
- (61) Tsukamoto, D.; Shiraishi, Y.; Sugano, Y.; Ichikawa, S.; Tanaka, S.; Hirai, T. Gold Nanoparticles Located at the Interface of Anatase/Rutile TiO_2 Particles as Active Plasmonic Photocatalysts for Aerobic Oxidation. *J. Am. Chem. Soc.* **2012**, *134*, 6309–6315.
- (62) Shiraishi, Y.; Sugano, Y.; Tanaka, S.; Hirai, T. One-Pot Synthesis of Benzimidazoles by Simultaneous Photocatalytic and Catalytic Reactions on Pt@ TiO_2 Nanoparticles. *Angew. Chem., Int. Ed.* **2010**, *49*, 1656–1660.
- (63) Sugano, Y.; Shiraishi, Y.; Tsukamoto, D.; Ichikawa, S.; Tanaka, S.; Hirai, T. Supported Au–Cu Bimetallic Alloy Nanoparticles: An Aerobic Oxidation Catalyst with Regenerable Activity by Visible-Light Irradiation. *Angew. Chem., Int. Ed.* **2013**, *52*, 5295–5299.
- (64) Shiraishi, Y.; Tanaka, K.; Shirakawa, E.; Sugano, Y.; Ichikawa, S.; Tanaka, S.; Hirai, T. Light-Triggered Self-Assembly of Gold Nanoparticles Based on Photoisomerization of Spirothiopyran. *Angew. Chem., Int. Ed.* **2013**, *52*, 8304–8308.
- (65) Shiraishi, Y.; Hirakawa, H.; Togawa, Y.; Hirai, T. Noble-Metal-Free Deoxygenation of Epoxides: Titanium Dioxide as a Photocatalytically Regenerable Electron-Transfer Catalyst. *ACS Catal.* **2014**, *4*, 1642–1649.
- (66) Shiraishi, Y.; Kanazawa, S.; Sugano, Y.; Tsukamoto, D.; Sakamoto, H.; Ichikawa, S.; Hirai, T. Highly Selective Production of Hydrogen Peroxide on Graphitic Carbon Nitride (g-C₃N₄) Photocatalyst Activated by Visible Light. *ACS Catal.* **2014**, *4*, 774–780.
- (67) Shiraishi, Y.; Kanazawa, S.; Kofuji, Y.; Sakamoto, H.; Ichikawa, S.; Tanaka, S.; Hirai, T. Sunlight-Driven Hydrogen Peroxide Production from Water and Molecular Oxygen by Metal-Free Photocatalysts. *Angew. Chem., Int. Ed.* **2014**, *53*, 13454–13459.